Siberia's largest pulse of kimberlites: U-Pb geochronology of perovskite and rutile from the Obnazhennaya kimberlite and its xenoliths, Siberia craton

Journal:	*International Geology Review*
Manuscript ID	TIGR-2021-0146.R3
Manuscript Type:	Data Article
Date Submitted by the Author:	n/a
Complete List of Authors:	Sun, Jing; China University of Petroleum Beijing, College of Geosciences Kostrovisky, Sergey; Institute of Geochemistry, Siberian Branch of the Russian Academy of Sciences, Irkutsk, Russia Mitchell, Ross; Institute of Geology and Geophysics Chinese Academy of Sciences Apen, Francisco; University of California Santa Barbara
Keywords:	perovskite, U-Pb geochronology, Obnazhennaya kimberlite, Siberia craton, rutile

Highlights

1. Obnazhennaya kimberlite age is 151.8±2.5 Ma, obtained by perovskite and rutile
2. It adds to the global "kimberlite bloom" from ca. 250–50 Ma
3. It is part of the largest kimberlite pulse of Siberia from ca. 171-144 Ma
4. Kimberlite pulse has spatiotemporal link to closure of the Mongol–Okhotsk Ocean
5. Closure of the MOO may act as a trigger for 171-144 Ma Siberia kimberlite pulse

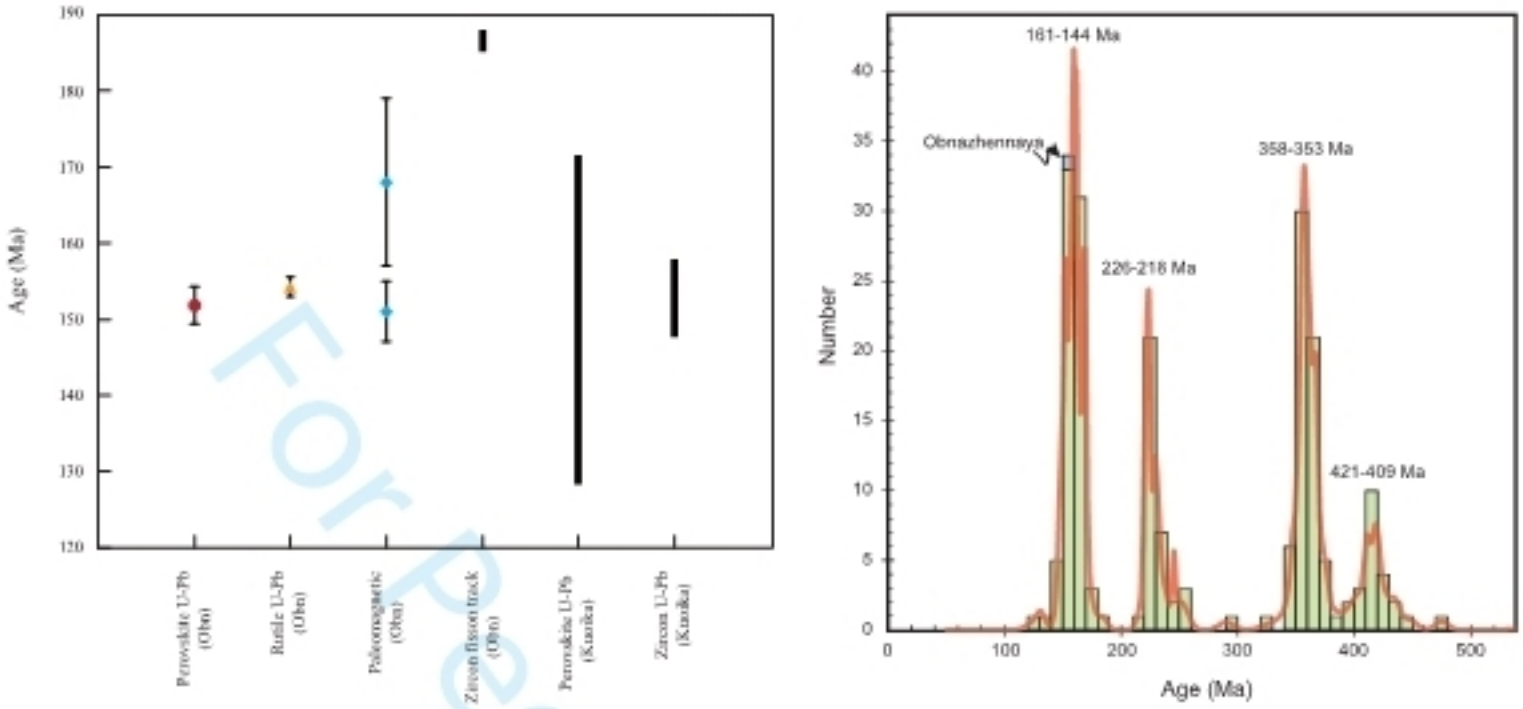
Age (Ma)
190
180
170
160
150
140
130
120
Perovskite U-Pb (Obn)
Rutile U-Pb (Obn)
Paleomagnetic (Obn)
Zircon fission track (Obn)
Perovskite U-Pb (Kuanika)
Zircon U-Pb (Kuanika)
161-144 Ma
Obnazhennaya
226-216 Ma
358-353 Ma
421-409 Ma
Number
40
35
30
25
20
15
10
5
0
0
100
200
300
400
500
Age (Ma)

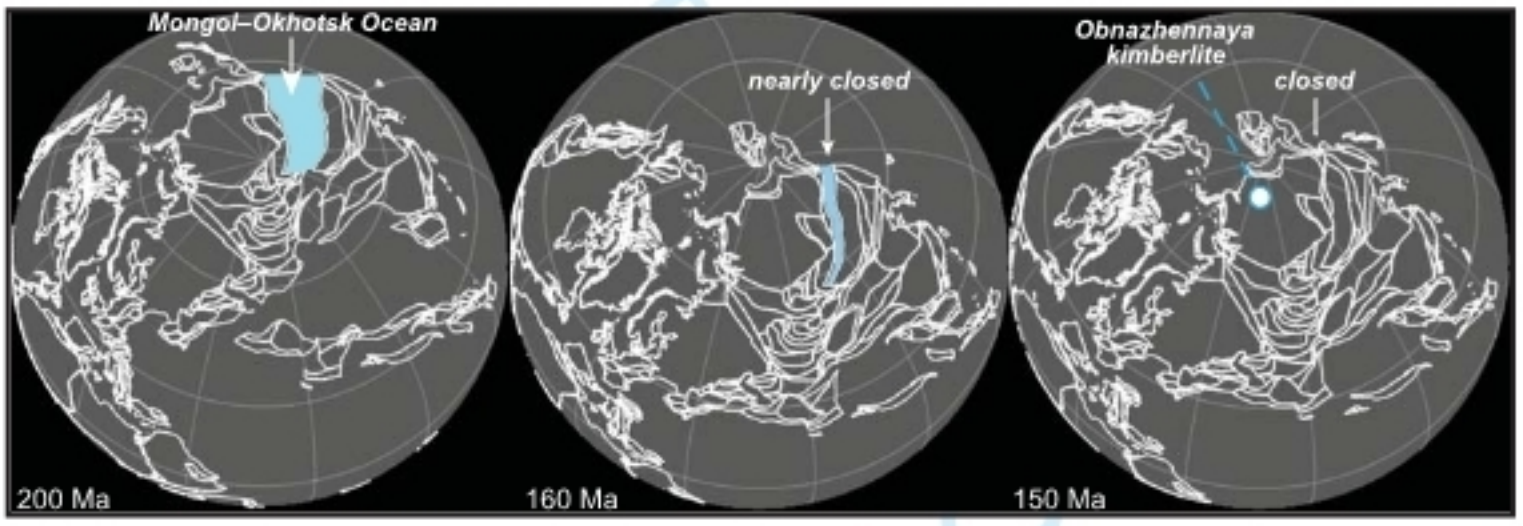
Mongol–Okhotsk Ocean
nearly closed
Obnazhennaya kimberlite
closed
200 Ma
160 Ma
150 Ma

Siberia's largest pulse of kimberlites: U-Pb geochronology of perovskite and rutile from the Obnazhennaya kimberlite and its xenoliths, Siberia craton

Jing Sun[1,2,*], Ross N. Mitchell[3], Sergey I. Kostrovitsky[4]

1 *State Key Laboratory of Petroleum Resources and Engineering， China University of Petroleum, Beijing, 102249, China*

2 *College of Geosciences, China University of Petroleum, Beijing, 102249, China*

3 *Institute of Geology and Geophysics, Chinese Academic of Science. 100029, Beijing, China.*

4 *Institute of Geochemistry, Siberian Branch of the Russian Academy of Sciences, Irkutsk, Russia*

***Corresponding author:**

Jing Sun

China university of Petroleum, Beijing

sunjing@cup.edu.cn

Abstract: Mantle xenoliths from the Obnazhennaya kimberlite are often compared with those from the Udachnaya kimberlite (ca. 367 Ma) to inform the evolution of the Siberia craton. However, the age of the Obnazhennaya kimberlite is unknown, and no reliable isotopic age estimates are available. Such uncertainty of the kimberlite age precludes a better understanding of the mantle xenoliths from the Obnazhennaya pipe, and thus also of the evolution of the Siberia craton. This paper reports U-Pb ages for both perovskite from the Obnazhennaya kimberlite and rutile in the Obnazhennaya eclogite xenoliths. The fresh perovskite with grain sizes of 30-90 μm formed during the early stage of magmatic crystallization. The perovskite U-Pb age is 151.8±2.5 Ma. Rutile has a lower closure temperature than its host eclogite. And its U-Pb isotope system was not closured until the host eclogite was extract by kimberlite. Hence, the rutile U-Pb age of 154.2±1.3 Ma can also represent the emplacement time of the Obnazhennaya kimberlite, and is within uncertainty of the perovskite U-Pb age. This first direct evidence for the emplacement age of the Obnazhennaya kimberlite adds to the global "kimberlite bloom" from ca. 250–50 Ma as well as the largest pulse of kimberlite volcanism in Siberia from ca. 171–144 Ma. The timing of this Jurassic–Cretaceous pulse coincides precisely with the closure of the Mongol–Okhotsk Ocean, but the depleted Sr-Nd isotopic characteristics of 171-144 Ma kimberlite challeng the directly subduction-related setting model of kimberlite petrogenesis, indicating the closure of the Mongol-Okhotsk ocean may act as a trigger of the initiation of 171-144 Ma kimberlite of Siberia.

Key words: perovskite; U-Pb geochronology; Obnazhennaya kimberlite; Siberia craton; rutile

1. Introduction

Kimberlite originates from the deep lithospheric mantle. During its emplacement up to the surface, kimberlites can entrain deep lithospheric mantle xenoliths that provide an opportunity to study the nature of the subcontinental lithospheric mantle (SCLM) beneath a craton (Li et al., 2010). The Siberia craton contains numerous kimberlite pipes, that entrained abundant mantle xenoliths. Studies on mantle xenoliths from the northern edge (Obnazhennaya) of the craton have strikingly different characteristics than those from the central craton (Udachnaya), both in terms of chemical composition, pressure-temperature and age (Howarth et al., 2014; Ionov et al., 2015a; Ionov et al., 2010, 2015b; Ionov et al., 2018; Pokhilenko et al., 1999; Sobolev 1974; Sobolev et al., 1984; Sun et al., 2017). Such contrasts may indicate a difference in lithospheric thickness up to 50 km between the two parts of the craton (Griffin et al., 1999). It is commonly thought that these characteristic differences reflect the evolution of the Siberia craton through time (Howarth et al., 2014; Ionov et al., 2015a; Ionov et al., 2010, 2015b; Ionov et al., 2018; Sobolev 1974; Sobolev et al., 1984; Sun et al., 2017). U-Pb dating of perovskite in kimberlite yields an eruption age of 367±5 Ma for the Udachnaya pipe (Kinny et al., 1997). However, no reliable isotopic age estimates are available for the Obnazhennaya kimberlite pipe. The emplacement age of this pipe is commonly assumed to be 160 Ma (Smelov and Zaitsev, 2013) because it belongs to the Kuoika kimberlite field. U-Pb dating of perovskite and zircon for several other pipes in the Kuoika field as well as those adjacent to the Obnazhennaya pipe range from 128 to 171 Ma (Davis et al., 1980; Griffin et al., 1999; Kinny et al., 1997; Sun et al., 2014; Sun et al., 2018). The majority of investigated kimberlite fields of the Yakutian province, Siberia, formed at the same episode, but multiple kimberlite magmatic events are known to have occurred within the same kimberlite field (Sun et al., 2014). For instance, the Ary-Mastah and Staraya Rechka fields of the Siberia craton both have Late Triassic and Middle/Late Jurassic kimberlite magmatism (Sun et al., 2014). Hence, it remains unknown when the Obnazhennaya kimberlite erupted.

Multiple methods have been used to date the Obnazhennaya kimberlite. K-Ar and Ar-Ar methods have most commonly been employed, but many factors may affect their reliability including the common alteration, low closure temperature, potential excess Ar, and the xenocrystic origin of some mica (Wu et al., 2010). Similar problems potentially exist for Rb-Sr dating of micas (e.g., Heaman et al., 2003; 2004). Perovskite occurs in many kimberlites worldwide. U-Pb isotope ratio analyses of perovskite have been suggested for dating kimberlites (Li et al., 2010; Sun et al., 2014; Yang et al., 2009, and references therein). However, perovskite usually occurs in kimberlites enriched in TiO_2 and FeO, which is inconsistent with the composition of the Obnazhennaya kimberlite (Kostrovitsky et al., 2007). Accessory minerals such as rutile in peridotite or eclogite xenoliths have low closure temperatures for Pb, thus U-Pb isotope ratio analyses of rutile typically yield ages similar to kimberlite emplacement ages as constrained independently from the perovskite groundmass phase (Schmitt et al., 2019).

Through detailed petrological and mineralological study of the Obnazhennaya kimberlite, we found perovskite in one of thirty kimberlite samples and rutile in one of twenty eclogite xenoliths. We have undertaken U-Pb isotope investigation by secondary ion mass spectrometry (SIMS) on perovskite from the Obnazhennaya kimberlite and laser ablation inductively coupled plasma mass spectrometry (LA-ICP-MS) on rutile from eclogite xenoliths from the Obnazhennaya kimberlite. Comparison of these new U-Pb ages with previously reported isotopic ages from the same kimberlite pipe enable us to definitively constrain the age of the Obnazhennaya kimberlite. This age will be helpful in constructing models for the evolution of the Siberia craton in future studies. Additionally, we consider how this new age compares with the distribution of kimberlites globally and in Siberia, as well as its relationship with the closure of the Mongol–Okhotsk Ocean.

2. Geological background and sample descriptions

The Siberia craton is larely covered by 2-14 km of Riphean (800-1600 Ma) to Lower Cretaceous sediments and Triassic traps; The Anabar and Aldan Precambrian

shield were outcropped. The Obnazhennaya kimberlite pipe of the Kuoika field is located within the lower Olenek province that occupies the northeastern most portion of the Siberia craton (Fig. 1). The Obnazhennaya kimberlite intruded Late Proterozoic limestone, dolomite and marl (Fig. 2 a, b), and its location along the tectonic margin of the craton during the late Permian has been suggested to reflect a mantle plume with the emplacement of the vast ca. 252 Ma (Burgess and Bowring, 2015) Siberian Traps large igneous province.

The majority of the Obnazhennaya pipe is high-Mg pyroclastic kimberlite, hypabyssal kimberlite inclusions are rarely to be found. Generally, the difference between pyroclastic and hypabyssal kimberlite is that the latter has higher FeO and TiO_2 contents. The chemical characteristics of Obnazhennaya kimberlite result in the lack of high-Ti, low-Cr assemblages of megacrysts, therefore, garnet, ilmenite, zircon and perovskite are rarely present in the Obnazhennaya kimberlite. Samples of perovskite-bearing kimberlite were collected. Thin sections were made and examined using scanning electron microscope-energy dispersive spectroscopy (SEM-EDS). Backscattered scanning electron (BSE) mode was utilized to image and confirm the presence perovskite. Perovskite grains exhibit various shapes, with subhedral to rounded grains being most common (Fig.2). Most perovskite grains are homogeneous in terms of major element composition and occur together with ilmenite. Perovskite grains with mineral inclusions were not analyzed. In general, the investigated perovskite grains are dark orange to brown in color and their grain sizes range between 30 μm and 90 μm.

The studied eclogite xenolith (obn74-968) from the Obnazhennaya kimberlite is coarse-grained and consists of garnet (56%), clinopyroxene (39%), and rutile (1%). Rutile grains with brownish color are observed as intergranular between garnet and clinopyroxene, inclusions of garnet or clinopyroxene, or exsolutions in garnet or clinopyroxene. Rutile grains are 30 to 100 μm in diameter, and only those larger than 60 μm were handpicked and mounted. Most mounted rutile grains are homogeneous in terms of major element compositions and exhibit rare ilmenite rims.

3. Analytical methods

Perovskite U-Pb analyses were conducted at the Institute of Geology and Geophysics, Chinese Academy of Sciences in Beijing. Approximately 5-mm-diameter plugs encompassing the perovskite were drilled out of a polished thin section and mounted in epoxy resin disks for SIMS analysis. The plugs were then imaged with a reflected light microscope to locate analytical spots for SIMS analysis. The sample mount was gold-coated prior to SIMS analysis. The U-Pb isotope systematics of perovskite in this study were analyzed by SIMS (CAMECA 1280), using the analytical procedure previously reported in Li et al. (2010). The O^{2-} primary ion beam was accelerated at 13 kV, with an intensity of 10^{-18} nA. Positive secondary ions were extracted with a 10 kV potential. Tazh perovskite was used as the primary standard to calibrate our U-Pb and Th-Pb data, and was measured after every six unknowns. The inverse (Tera-Wasserburg) Concordia diagram was used to obtain ages, from the lower-grain fractions, assuming the initial common lead isotope composition follows the Stacey and Kramers (1975) model (SK model Pb isotopes, or ^{207}Pb correction). For our SIMS U-Pb data, we also corrected for the presence of initial common Pb based on the measured ^{204}Pb contents, and the ^{204}Pb-corrected ages are identical within uncertainty to the ^{207}Pb-corrected ages. All initial common-Pb-corrected and weighted average $^{206}Pb/^{238}U$ ages were calculated using ISOPLOT 3.0 (Ludwig, 2003). Uncertainties on individual analyses and pooled ages are reported at the 2σ level. During the analytical sessions, the AFK perovskite was repeatedly analyzed as an unknown and the analyses of this in-house standard yielded a weighted average $^{206}Pb/^{238}U$ age of 385.5±8.4 Ma (MSWD=2.9, *n=8*), which is identical to the TIMS age of 381.6±1.4 Ma (Wu et al., 2013).

Measurements of U-Pb isotopes were performed using a Photon Machines 193 nm Excimer laser ablation system coupled to a Nu Instruments Attom high-resolution sector-field ICP-MS at the University of California, Santa Barbara. Rutile crystals were mounted in a transparent epoxy and the mount was polished to expose the fresh interior of the crystal. Detailed methods are described in Kooijman et al. (2017). Analyses were achieved using 7 mJ and 4 Hz for 16s on 30 μm-wide spots. The Pb/U

ratios were normalized to R9826J standard rutile (381.9±1.1 Ma; Kylander-Clark et al., 2008), which was reproduced to within 0.12% relative standard deviation. Accuracy was assessed by analyzing KRAG1 and WOD, for which we obtained $^{206}Pb/^{238}U$ ages of 1092±13 Ma (*n*=*7*) and 2817±36 Ma (*n*=*8*) for these materials, respectively, thus demonstrating accuracy to within 1%.

4. Results

4.1 SIMS U-Pb ages of perovskite

The U-Pb isotope data of perovskite grains from the Obnazhennaya kimberlite are listed in Supp. Table 1. As shown by SIMS data, the perovskite grains have high U (28-53 ppm) and Th (61-2037 ppm) contents that are favorable for U-Pb age determinations. However, the high Pb contents require a common lead correction. Typically, common Pb corrections to perovskite data have been made using the 207Pb correction method or the Tera-Wasserburg diagram

Twenty-five analyses define a discordia line with a lower intercept age of 151.8±1.8 Ma on the Tera-Wasserburg diagram (Fig. 3a), if an initial common lead composition is assumed according to the model of Stacey and Kramers (1975). $^{207}Pb/^{206}Pb$ ratios of these perovskite grains range from 0.271 to 0.334. The $^{206}Pb/^{238}U$ weighted average age is 151.8±2.5 Ma with ^{207}Pb correction (Fig. 3b).

4.2 LA-ICPMS U-Pb ages of rutile

The U-Pb isotope data of rutile grains from eclogite xenoliths of the Obnazhennaya kimberlite are listed in Supp. Table 2. A total of eighteen analyses were conducted on 11 rutile grains with diameters about 60 μm (the largest grain up to 100 μm). The measured U contents range from 1.1 to 6.8 ppm, mostly >4 ppm. On the Tera-Wasserburg plot, linear regression of the data points (MSWD=1.16) gives a lower intercept age of 153.8±1.6 Ma (Fig. 3c). A weighted mean $^{206}Pb/^{238}U$ age is 154.2±1.3 Ma (Fig. 3d) using the ^{207}Pb-based common-lead correction with the terrestrial Pb isotope composition of Stacey and Kramers (1975), which is consistent with the lower intercept age within errors.

5. Discussion

The Obnazhennaya kimberlite pipe is widely considered one of the most important pipes to study the evolution of Siberia craton (Howarth et al., 2014; Ionov et al., 2015a; Ionov et al., 2018; Sun et al., 2017; Taylor et al., 2003). This is because it contains mantle xenoliths of eclogites, pyroxenites, and peridotites that can be used to reflect the characteristics of the SCLM beneath the craton. In interbedded sedimentary layers, the kimberlite contains *Belemnite rostra* (Milashev and Shul'gina, 1959; Malkov and Gustomesov, 1976) and wood remnants (Kostrovitsky and Admakin, 1991) from the Late Jurassic, indicating the emplacement age is not younger than Late Jurassic. However, precise isotopic age data for this kimberlite are lacking and only a few techniques were applied during the past four decades (Fig. 4). Using the K-Ar technique, Brakhfogel (1984) obtained an age of 418±14 Ma. But many factors including the common alteration, low closure temperature, potential excess Ar, and the xenocrystic origin of the analyzed mica may affect such data and therefore this result is treated with caution (Sun et al., 2014). Using paleomagnetism, two possible ages (168±11 and 151±4 Ma) were provided by Blanco et al. (2013) based on different apparent polar wander paths. An age of 185-188 Ma for the Obnazhennaya kimberlite was also obtained from zircon fission tracks (Griffin et al., 1999). In summary, the majority of available age data range from 151 to 185 Ma, with an unusually old age of 418 Ma. These data are not precise and reliable enough to constrain the emplacement age of the Obnazhennaya kimberlite.

It has been demonstrated that perovskite and mantle zircon megacrysts are good for dating kimberlites with U-Pb geochronology. Perovskite crystallizes at a relatively early stage form a kimberlite magma and contains enough U for precise Pb isotopic analyses, and hence redindering it reliable for U-Pb age determination (e.g., Kinny et al., 1997; Li et al., 2010; Yang et al., 2009; Sun et al., 2014). As for mantle zircon, they are typically interpreted as high-pressure crystals that precipitated directly from kimberlite melt (Moore and Belousova, 2005). The crystallization environment in the lower cratonic lithosphere is near the closure temperature for Pb in zircon (~1000°C;

Mezger and Krogstad, 1997), thus mantle zircon typically yields ages similar to kimberlite magma emplacement ages as well as perovskite (Castillo-Oliver et al., 2016; Robles-Cruz et al., 2012).

U-Pb ages on zircon and perovskite from other pipes in the Kuoika field have given ages of 148-157 Ma (Brakhfogel, 1984; Davis et al., 1980; Griffin et al., 1999; Lepekhina et al., 2008; Sun et al., 2018) and 128-171 Ma (Bristow et al., 1991; Heaman and Mitchell, 1995; Kinny et al., 1997; Sun et al., 2014), respectively (Fig. 4). Therefore, Middle/Late Jurassic kimberlite emplacement ages have been suggested for all kimberlite pipes in the Kuoika field. Although the majority of investigated kimberlite fields from the Siberia craton formed over a relatively short time interval of <30 Myr, some kimberlite fields of the craton have multiple kimberlite magmatic events, as occurred within the Ary-Mastah (ca. 231-216 Ma and ca. 170-165 Ma) and Staraya Rechka (ca. 224-220 Ma and ca. 169-162 Ma) kimberlite fields (Sun et al., 2014).

In this study, thirty samples were selected for perovskite U-Pb isotopic analyses. However, only one sample, Obn 7-191, was found to contain perovskite, confirming that perovskite is rare in the Obnazhennaya kimberlite, which is characterized by high Mg and low Ti, Fe and K contents. The weighted perovskite U-Pb age of sample Obn 7-191 is 151.8 ± 2.5 Ma (*n=25*). We consider this age to be the best estimate of the emplacement time of the Obnazhennaya kimberlite.

The rutile U-Pb measurements show relatively high U content (>1 ppm). Li et al. (2011) has suggested that rutile grains with low U (<1 ppm) cannot be measured accurately. In contrast, an accurate age is attainable when grains have U contents higher than 1 ppm. A pooled analysis of all 18 measurements on rutile yields lower intercept age on a Tera-Wasserburg plot of 153.8±1.6 Ma (MSWD=1.2), which is interpreted as the best estimate for the rutile U-Pb age. Rutile occurs widely in eclogites, however, the interpretation of rutile U-Pb ages is not straightforward due to the uncertainty of the U-Pb closure temperature (T_c). Field-based studies on rutile from slowly cooled rocks imply that the T_c for rutile in the U-Pb system is ~400-500°C (Mezger et al., 1989). However, Cherniak (2000) suggests that T_c is

~600°C for rutile grains of ~0.1 mm under dry conditions and higher than 600°C under wet conditions based on lead diffusion. Kooijman et al. (2010) demonstrate that it is impossible to define one single temperature for the closure of Pb in rutile, where rutile has a variable T_c ranging from ~640°C in the core to ~490°C in the rim. Compared with the eclogites, the T_c of rutile is at least 150°C lower than the equilibration temperatures of 800-1000°C(Sun unpublished data). Therefore, the U-Pb system of rutile in eclogites was open until the kimberlite extracted and transported eclogites to the surface. The rutile U-Pb age is consistent with the perovskite U-Pb age of 151.8±2.5 Ma from kimberlite, strongly suggesting that the emplacement time of the Obnazhennaya kimberlite occurred 9 Myr younger than previous estimates (Smelov and Zaitsev, 2013). A Late Jurassic age for the Obnazhennaya kimberlite places it within the "kimberlite bloom" between ca. 250 and 50 Ma that accounts for >60% of all known kimberlites worldwide (Tappe et al. 2018). Our precise age for the important Obnazhennaya kimberlite will play critically into revising models for the tectonic evolution of the Siberia craton. Hence, the mantle xenoliths from the Obnazhennaya kimberlite reflect the lithospheric mantle characteristics at 151 Ma, and the mantle xenoliths from Udachnaya and Obnazhennaya indicate the evolution of the Siberia craton from 367 to 151 Ma.

In addition to fitting within the longer global "kimberlite bloom", our 151 Ma age for the Obnazhennaya kimberlite places it within the late Jurassic to early Cretaceous (171–144 Ma) kimberlite pulse of the Siberia craton itself (Sun et al., 2018). This is the largest pulse of kimberlite volcanism for the craton throughout its history, even among the multiple significant Phanerozoic pulses (Fig. 5). We consider whether the tectonic setting of this particular age may have played a role in promoting this superlative pulse of kimberlites in Siberia. The interval in question is notable for the final closure of the Mongol–Okhotsk Ocean (MOO) between Siberia and Amuria (Fig. 6). Initially ~4,700 km wide in the Permian, the MOO was slightly reduced in size during the Triassic, but a remaining large tract of ~2,650 km is thought to have closed in the Jurassic and early Cretaceous (Kravchinsky et al., 2002; Wu et al., 2017). Furthermore, a seismically imaged slab "graveyard" has been located beneath Siberia

near the core–mantle boundary and is interpreted as the remnants of the prolific episode of subduction occurring ~150 million years ago (Van der Voo et al., 1999). As Siberia was the upper plate during the convergence, slab dehydration and decarbonation may account for the pulse of kimberlite volcanism occurring at precisely the same time as so much of the MOO closure so quickly (Fig. 6). The tectonic setting of the rapid closure of the MOO beneath may thus provide support for models of kimberlite petrogenesis involving the deep subduction (Stern et al., 2016). However, the Sr-Nd isotopic compositions of 171-144 Ma kimberlite of Siberia (Sun et al., 2018) is relatively depleted, i.e., the subducted oceanic crust and sediments did not contribute to the Siberia kimberlitic magma, which challenges the directly subduction-related setting model. Therefore, the closure of Mongol-Okhotsk Ocean may only act as a trigger for the initiation of 171-141 Ma kimberlite of Siberia.

6. Conclusion

A precise perovskite U-Pb age provides the first direct evidence for the emplacement age of the Obnazhennaya kimberlite. The perovskite U-Pb age from kimberlite is corroborated by a rutile U-Pb age of 151.8±2.5 Ma from eclogite xenoliths of the Obnazhennaya kimberlite. This age falls within and thus adds to a well-known age for kimberlite volcanism worldwide, as well as adding to the most significant pulse of kimberlites in the history of Siberia itself. The exact timing of this igneous activity coincides precisely with the subduction of the Mongol–Okhotsk Ocean beneath Siberia, but the depleted Sr-Nd isotopic characteristics of 171-144 Ma kimberlite challenges the directly subduction-related setting model of kimberlite petrogenesis, indicating that the closure of Mongol-Okhotsk Ocean may only act as a trigger for the initiation of 171-144 Ma kimberlite of Siberia.

Acknowledgement

This study was supported by a grant from the National Natural Science Foundation of China (42072060).

References

Blanco, D., Kravchinsky, V.A., Konstantinov, K.M., and Kabin, K., 2013, Paleomagnetic dating of Phanerozoic kimberlites in Siberia. Journal of Applied Geophysics, v. 88, p.139-153.

Brakhfogel, F.F., 1984, Geological aspects of kimberlite magmatism in the northeastern Siberian Platform (in Russian). Yakutian of SO AN USSR Press, Yakutsk, pp.128.

Bristow, J.W., Barton, E.S., Compston, W., Williams, I.S., and Smith, C.B., 1991, Determination of kimberlite and related-rock emplacement ages by ion-microprobe analysis of in situ perovskites. In proceedings of the 5th Kimberlite Conference, Araxa, Brazil.

Burgess, S.D., and Bowring, S.A., 2015, High-precision geochronology confirms voluminous magmatism before, during, and after Earth's most severe extinction. Science Advance, v.1, e1500470.

Castillo-Oliver, M., Galí, S., Melgarejo, J.C., Griffin, W.L., Belousova, E., Pearson, N.J., Watangua, M., and O'Reilly, S.Y., 2016, Trace-element geochemistry and U–Pb dating of perovskite in kimberlites of the Lunda Norte province (NE Angola): Petrogenetic and tectonic implications. Chemical Geology, v. 426, p.118-134.

Cherniak, D.J., 2000, Pb diffusion in rutile. Contributions to Mineralogy and Petrology, v.139, p.198-207.

Davis, G.L., Sobolev, N.V., and Khar'Kiv, A.D., 1980, New data on the age of Yakutian kimberlites obtained by the uranium-lead on zircons. Dokl. Akad. Nauk SSSR, v.254, p.175-180.

Griffin, W.L., Ryan, C.G., Kaminsky, F.V., O'Reilly, S.Y., Natapov, L.M., Win, T.T., Kinny, P.D., and Ilupin, I.P., 1999, The Siberian lithosphere traverse: mantle terranes and the assembly of the Siberian Craton. Tectonophysics, v.310, p.1-35.

Heaman, L.M., Kjarsgaard, B.A., and Creaser, R.A., 2003, The timing of kimberlite magmatism in North America: Implications for global kimberlite genesis and diamond exploration. Lithos, v.71, p.153-184.

Heaman, L.M., Kjarsgaard, B.A., and Creaser, R.A., 2004, The temporal evolution of North American kimberlites. Lithos, v.76, p.377-397.

Heaman, L.M., and Mitchell, R.H., 1995, Constraints on the emplacement age of Yakutian province kimberlites from U-Pb perovskite dating. In proceedings of the 6_{th} International

Kimberlite Conference, Novosibirsk, Russi, 233.

Howarth, G.H., Barry, P.H., Pernet-Fisher, J.F., Baziotis, I.P., Pokhilenko, N.P., Pokhilenko, L.N., Bodnar, R.J., Taylor, L.A., and Agashev, A.M., 2014, Superplume metasomatism: Evidence from Siberian mantle xenoliths. Lithos, v.184–187, p. 209-224.

Ionov, D.A., Carlson, R.W., Doucet, L.S., Golovin, A.V., and Oleinikov, O.B., 2015a, The age and history of the lithospheric mantle of the Siberian craton: Re–Os and PGE study of peridotite xenoliths from the Obnazhennaya kimberlite. Earth and Planetary Science Letters, v.428, p. 108-119.

Ionov, D.A., Doucet, L.S., and Ashchepkov, I.V. 2010, Composition of the lithospheric mantle in the siberian craton: new constraints from fresh peridotites in the udachnaya-east kimberlite. Journal of Petrology, v.51(11), p. 2177-2210.

Ionov, D.A., Doucet, L.S., and Ashchepkov, I.V., 2015b, Post-Archean formation of the lithospheric mantle in the central Siberian craton: Re–Os and PGE study of peridotite xenoliths from the Udachnaya kimberlite. Geochimica Et Cosmochimica Acta, v.165, p.466-483.

Ionov, D.A., Doucet, L.S., Xu, Y., Golovin, A.V., and Oleinikov, O.B., 2018, Reworking of Archean mantle in the NE Siberian craton by carbonatite and silicate melt metasomatism: Evidence from a carbonate-bearing, dunite-to-websterite xenolith suite from the Obnazhennaya kimberlite. Geochimica Et Cosmochimica Acta, v.224, p.132-153.

Kinny, P.D., Griffin, B., Heaman, L., Brakhfogel, F., and Spetsius, Z.V., 1997, SHRIMP U-Pb ages of perovskite from Yakutian kimberlites. Russian Geology and Geophysics C/C of Geologia I Geofizifa, v.38, p.97-105.

Kooijma, E., Smit, M.A., Mezger, K., Ratschbacher, L., and Kylander-Clark, A.R.C., 2017, A view into crustal evolution at mantle depths. Earth and Planetary Science Letters, v.465, p.59-69.

Kostrovitsky, S.I., and Admakin, L.A., 1991, A find of xenolithic wood remnants in the Obnazhennaya kimberlite pipe. Russian Geology and Geophysics, v.32 (11), p.82-84.

Kostrovitsky, S.I., Morikiyo, T., Serov, I.V., Yakovlev, D.A., and Amirzhanov, A.A., 2007, Isotope-geochemical systematics of kimberlites and related rocks from the Siberian Platform. Russian Geology and Geophysics, v.48, p.272-290.

Kravchinsky, V.A., Cogn, J.P., Harbert, W.P., and Kuzmin, M.I., 2010, Evolution of the Mongol-Okhotsk ocean as constrained by new Palaeomagnetic data from the Mongol-Okhotsk suture zone, Siberia. Geophysical Journal of the Royal Astronomical Society, v.148(1), p.34-57.

Kylander-Clark, A.R.C., Hacker, B.R., and Mattinson, J.M., 2008, Slow exhumation of UHP terranes: Titanite and rutile ages of the Western Gneiss Region, Norway. Earth and Planetary Science Letters, v.272, p.531-540.

Lepekhina, E.N., Rotman, A.Y., Antonov, A.V., and Segeev, S.A., 2008, SHRIMP U-Pb dating of perovskite from kimberlites of Siberian platform (Verkhnyaya Muna and Alakit-Markha Fields). In proceedings of the 9th International Kimberlite Conference, Frankfurt, Germany, 00353.

Li, Q.L., Li, X.H., Liu, Y., Wu, F.Y., Yang, J.H., and Mitchell, R.H., 2010, Precise U–Pb and Th–Pb age determination of kimberlitic perovskites by secondary ion mass spectrometry. Chemical Geology, v.269, p.396-405.

Li, Q.L., Lin, W., Su, W., Li, X.H., Shi, Y.H., Liu, Y., and Tang, G.Q., 2011, SIMS U-Pb rutile age of low temperature eclogites from southwestern Chinese Tianshan, NW China. Lithos, v.122(1), p.76-86.

Ludwig, K.R., 2003, ISOPLOT 3.0-a geochronological toolkit for Microsoft Excel, Berkeley Geochronology Center Special Publication.

Malkov, B.A., and Gustomesov, V.A., 1976, Jurassic fauna in kimberlites from the Olenek uplift and the age of kimberlite pyrosm in the northeastern Siberian craton. DAN SSSR, v.229(2), p.435-438.

Mezger, K., and Krogstad, E.J., 1997, Interpretation of discordant U-Pb zircon ages: An evaluation. Journal of Metamorphic Geology, v.15(1), p.127-140.

Milashev, V.A., and Shul'gina, N.I., 1959, New data on the age of the kimberlites of the Siberian Platform: Doklady Akad (in Russian). Nauk SSSR, v.126, p.1320-1322.

Moore, A., and Belousova, E., 2005, Crystallization of Cr-poor and Cr-rich megacryst suites from the host kimberlite magma: implications for mantle structure and the generation of kimberlite magmas. Contributions to Mineralogy and Petrology, v.149, p.462-481.

Pokhilenko, N., Sobolev, N.V., Kuligin, S.S., and Shimizu, N., 1999, Peculiarities of distribution

of pyroxenite paragenesis garnets in Yakutian kimberlite and some aspects of the evolution of the Siberian Craton lithosphericmantle. Proceedings of the VIIth International Kimberlite Conference, 689-698.

Robles-Cruz, S.E., Escayola, M., Jackson, S., Gali, S., Pervov, V., Watangua, M., Goncalves, A., and Melgarejo, J.C., 2012, U-Pb SHRIMP geochronology of zircon from the Catoca kimberlite, Angola: Implications for diamond exploration. Chemical Geology, v.310, p.137-147.

Schmitt, A.K., Zack, T., Kooijman, E., Logvinova, A., and Sobolev, N.V., 2019, U-Pb ages of rare rutile inclusions in diamond indicate entrapment synchronous with kimberlite formation. Lithos, v.350-351, p.105251-.

Smelov, A.P., and Zaitsev, A.I., 2013, The Age and Localization of Kimberlite Magmatism in the Yakutian Kimberlite Province. Constraints from Isotope Geochronology—An Overview. Springer India.

Sobolev, N.V., 1974, Deep-Seated Inclusions in Kimberlites and the Problem of the Composition of the Mantle. Amer. Geophys. Union. Washington, DC. pp 279.

Sobolev, N.V., Pokhilenko, N.V., and Efimova, E.S., 1984, Xenoliths of diamond bearing peridotites in kimberlites and problem of the diamond origin. Russian Geology and Geophysics, v.25 (12), p.63–80.

Stacey, J.S., and Kramers, J.D., 1975, Approximation of terrestrial lead isotope evolution by a two-stage model. Earth and Planetary Science Letters, v.26, p.207-221.

Stern, R.J., Leybourne, M.I., and Tsujimori, T., 2016, Kimberlites and the start of plate tectonics. Geology, v.44(10), p.799-802.

Sun, J., Liu, C.Z., I. Kostrovisky, S., Wu, F.Y., Yang, J.H., Chu, Z.Y., Yang, Y.H., Kalashnikova, T., and Fan, S., 2017, Composition of the Lithospheric Mantle in the Northern part of Siberian Craton: Constraints from Peridotites in the Obnazhennaya Kimberlite. Lithos, v.294, p.383-396.

Sun, J., Liu, C.Z., Tappe, S., Kostrovitsky, S.I., Wu, F.Y., Yakovlev, D., Yang, Y.H., and Yang, J.H., 2014, Repeated kimberlite magmatism beneath Yakutia and its relationship to Siberian flood volcanism: Insights from in situ U–Pb and Sr–Nd perovskite isotope analysis. Earth and Planetary Science Letters, v.404, p.283–295.

Sun, J., Tappe, S., Kostrovitsky, S.I., Liu, C.Z., Skuzovatov, S.Y., and Wu, F.Y., 2018, Mantle sources of kimberlites through time: A U-Pb and Lu-Hf isotope study of zircon megacrysts from the Siberian diamond fields. Chemical Geology, v.479, p.228-240.

Tappe, S., Smart, K., Torsvik, T., Massuyeau, M., and de Wit, M., 2018, Geodynamics of kimberlites on a cooling Earth: Clues to plate tectonic evolution and deep volatile cycles. Earth and Planetary Science Letters, v.484, p.1-14.

Taylor, L.A., Snyder, G.A., Keller, R., Remley, D.A., Anand, M., Wiesli, R., Valley, J., and Sobolev, N.V., 2003, Petrogenesis of group A eclogites and websterites: Evidence from the Obnazhennaya kimberlite, Yakutia. Contributions to Mineralogy and Petrology, v.145, p.424-443.

Van, der, V.R, Spakman, W., and Bijwaard, H., 1999, Mesozoic subducted slabs under siberia. Nature v.397, p.246-249.

Wu, F.Y., Arzamastsev, A.A., Mitchell, R.H., Li, Q.L., Sun, J., Yang, Y.H., and Wang, R.C., 2013, Emplacement age and Sr-Nd isotopic compositions of the Afrikanda alkaline ultramafic complex, Kola Peninsula, Russia. Chemical Geology, v.353, p.210-229.

Wu, F.Y., Yang, Y.H., Mitchell, H.R., Li, Q.L., Yang, J.H., and Zhang, Y.B., 2010, In situ U-Pb age determination and Nd isotopic analysis of perovskites from kimberlites in southern Africa and Somerset Island, Canada. Lithos, v.115, p.205-222.

Wu, L., Kravchinsky, V.A., and Potter, D.K., 2017, Apparent polar wander paths of the major chinese blocks since the late paleozoic: toward restoring the amalgamation history of east eurasia. Earth-Science Reviews, 492-519.

Yang, Y.H., Wu, F.Y., Wilde, S.A., Liu, X.M., Zhang, Y.B., Xie, L.W., and Yang, J.H., 2009, In situ perovskite Sr-Nd isotopic constraints on the petrogenesis of the Ordovician Mengyin kimberlites in the North China Craton. Chemical Geology, v.264, p.24-42.

Figure captions

Fig.1 Overview map of the Siberia craton (**a**) and the Kuoika kimberlite field (**b**), showing the location of the Obnazhennaya kimberlite pipes. LIP: Large igneous province. Fig.1**a** is modified from Howarth et al. (2014).

Fig.2 Photos of Obnazhennaya kimberlite pipe field (**a-b**). BSE images of perovskite crystals from the Obnazhennaya kimberlite (**c-d**) and rutile crystals in eclogite xenoliths of the Obnazhennaya kimberlite (**e-f**). Prv. perovskite; Ilm. ilmenite; Phl. phlogopite; Opx. orthorpyroxene; Cpx. clinopyroxene. Scale bar is 20 μm.

Fig.3 U-Pb isotopic ages of perovskite grains from the Obnazhennaya kimberlite (**a, b**) and rutile grains from eclogite xenoliths of the Obnazhennaya kimberlite (**c, d**). The upper intercepts (**a, c**) are fixed at the common Pb composition from the terrestrial Pb isotope evolution model of Stacey and Kramers (1975), i.e., SK model, and a regression line is forced through the uncorrected U-Pb data and the SK common Pb composition to obtain the lower intercept age. The $^{206}Pb/^{238}U$ weighted ages (**b**, **d**) were calculated after ^{207}Pb correction calculated using the SK common Pb composition.

Fig.4 Comparison of all available ages for kimberlites from the Obnazhennaya pipe and the Kuoika kimberlite field. Paleomagnetic data of the Obnazhennaya kimberlite is from Blanco et al. (2013). Not shown is Obnazhennaya kimberlite K-Ar data of 400 Ma (Brakhfogel 1984). Zircon fission track data of Obnazhennaya kimberlite is from Griffin et al. (1999). U-Pb ages of zircon and perovskite from the Kuoika kimberlite field are from Brakhfogel (1984); Bristow et al. (1991); Davis et al. (1980); Griffin et al. (1999); Kinny et al. (1997); Lepekhina et al. (2008); Sun et al. (2014); Sun et al. (2018).

Fig.5 Frequency histogram (light green and light blue) and probability density (red) function of Siberian kimberlites. Light green represent Siberian kimberlite ages in previous studies, data are from Griffin et al. (1999), Davis et al. (1980), Lepekhnia et al. (2008), Sun et al.(2014) and Sun et al. (2018). Light blue represents U-Pb age for perovskite from Obnazhennaya kimberlite.

Fig.6 Paleoreconstructions of Mongol-Okhotsk Ocean (MOO) from 200 Ma to 150 Ma. Light blue represents the Mongol Okhotsk Ocean (MOO).

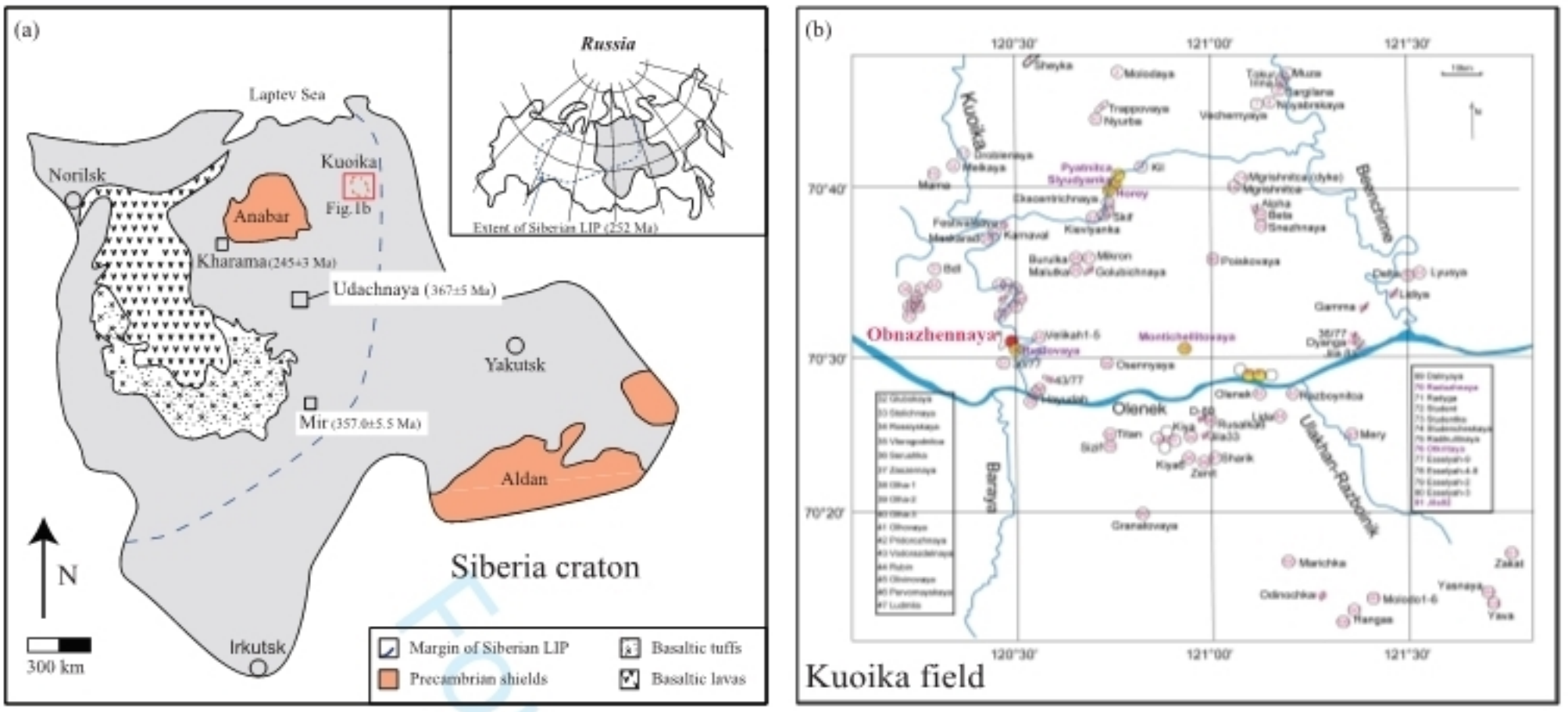

Fig.1

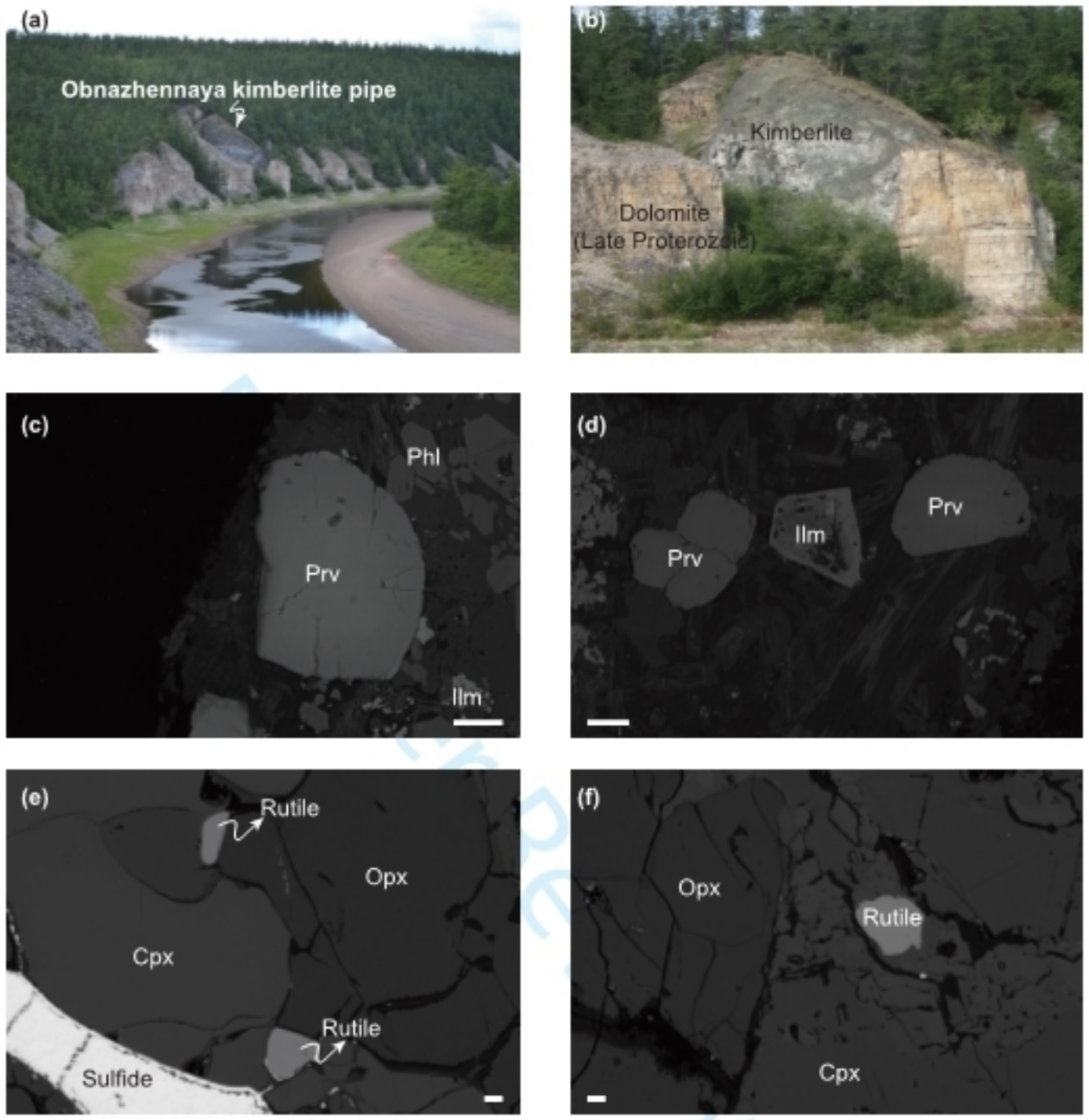
(a)
Obnazhennaya kimberlite pipe
(b)
Kimberlite
Dolomite
(Late Proterozoic)
(c)
Phl
Prv
Ilm
(d)
Prv
Ilm
Prv
(e)
Rutile
Opx
Cpx
Rutile
Sulfide
(f)
Opx
Rutile
Cpx

Fig.2

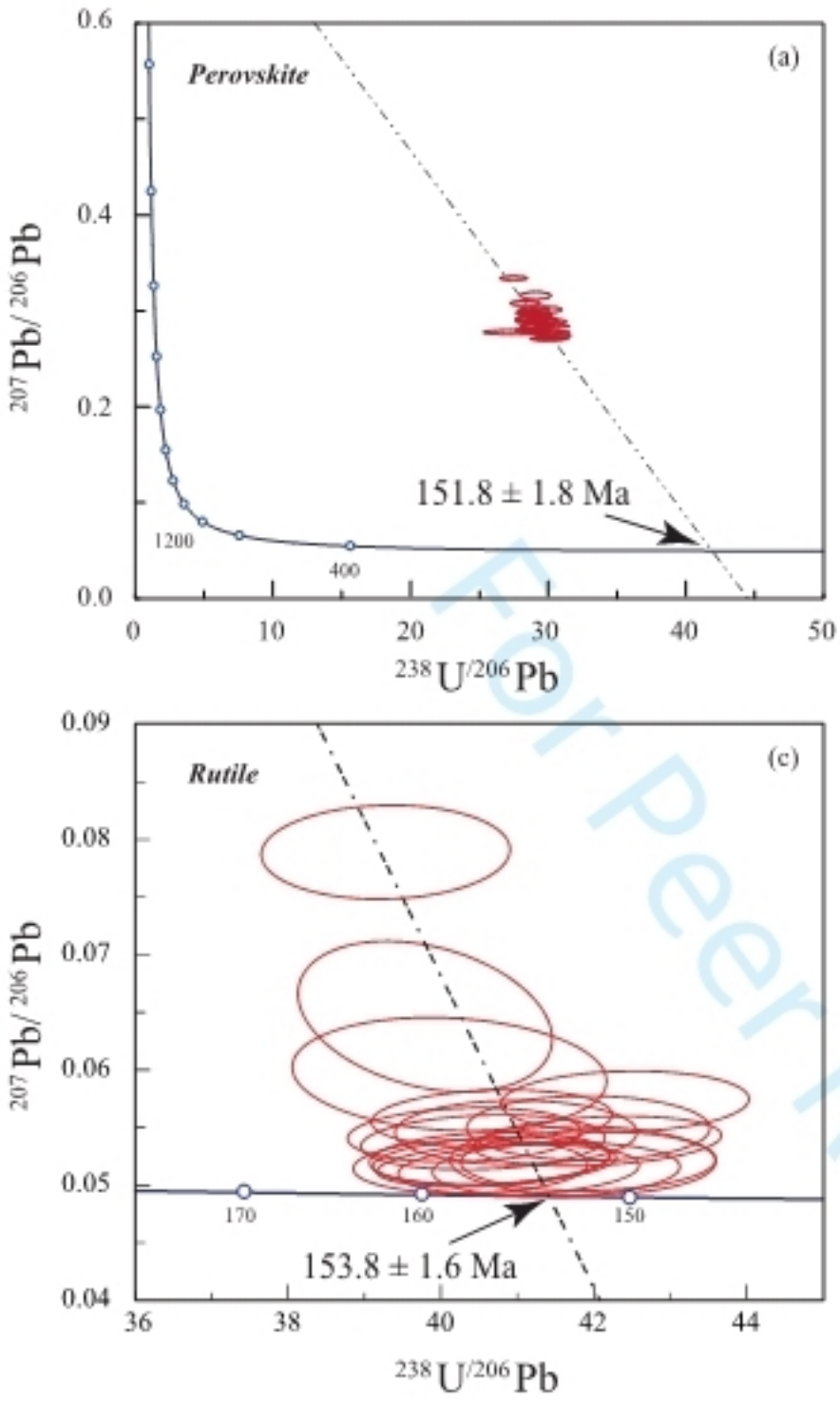
Perovskite
(a)
151.8 ± 1.8 Ma
1200
400
$^{207}Pb/^{206}Pb$
$^{238}U/^{206}Pb$
Rutile
(c)
153.8 ± 1.6 Ma
170
160
150

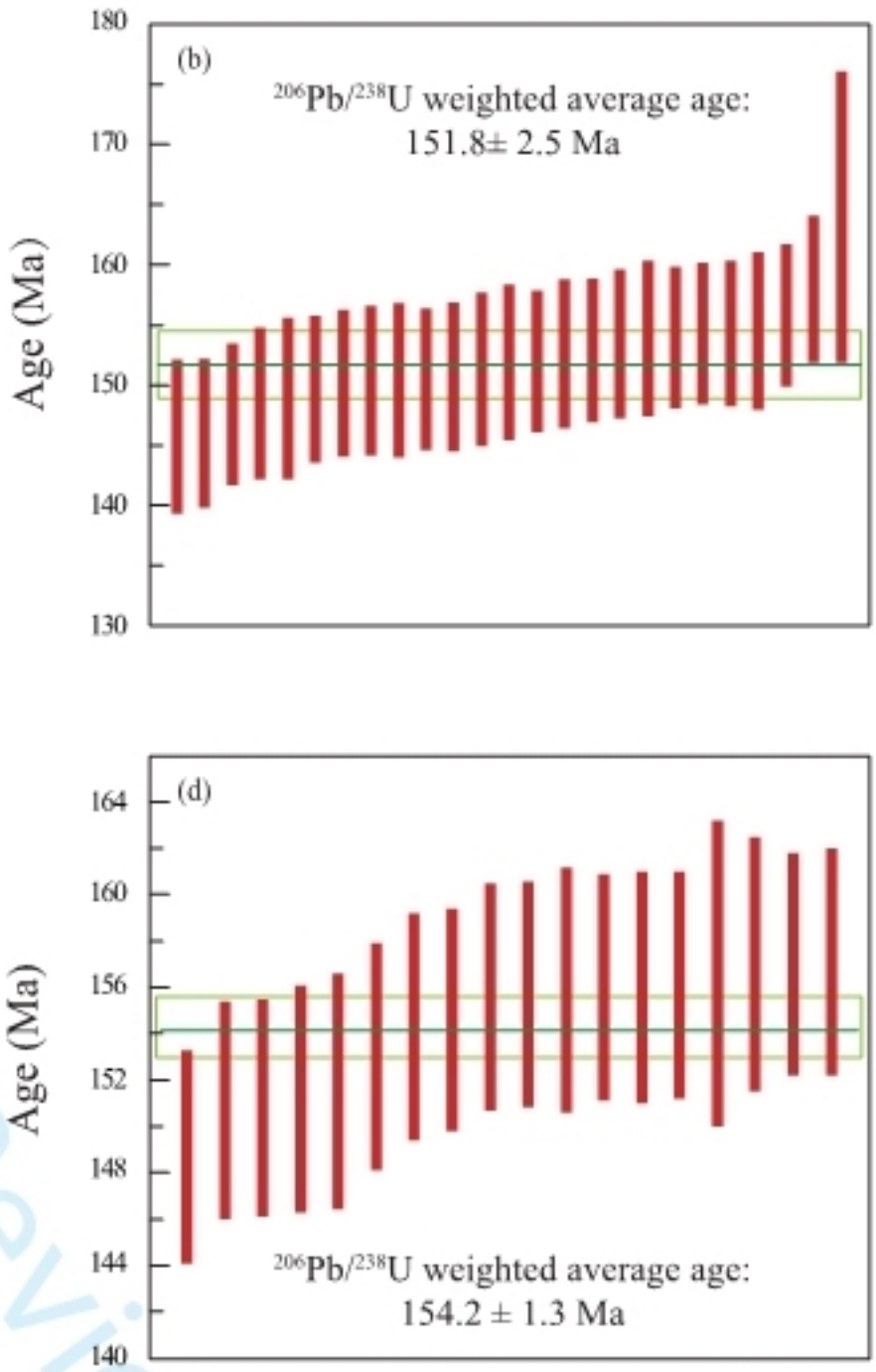
(b)
$^{206}Pb/^{238}U$ weighted average age:
151.8± 2.5 Ma
Age (Ma)
(d)
$^{206}Pb/^{238}U$ weighted average age:
154.2 ± 1.3 Ma

Fig. 3

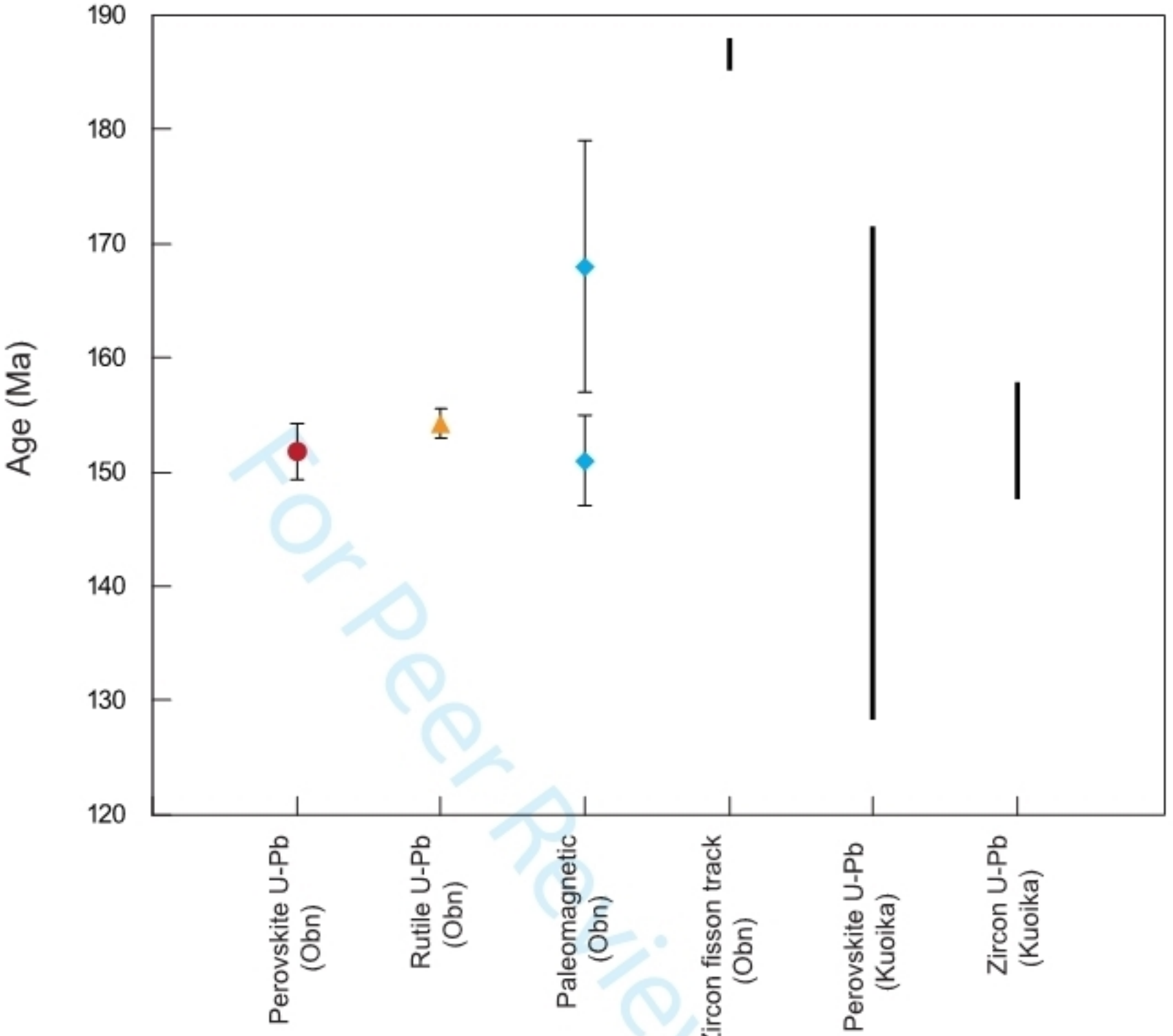

Fig. 4

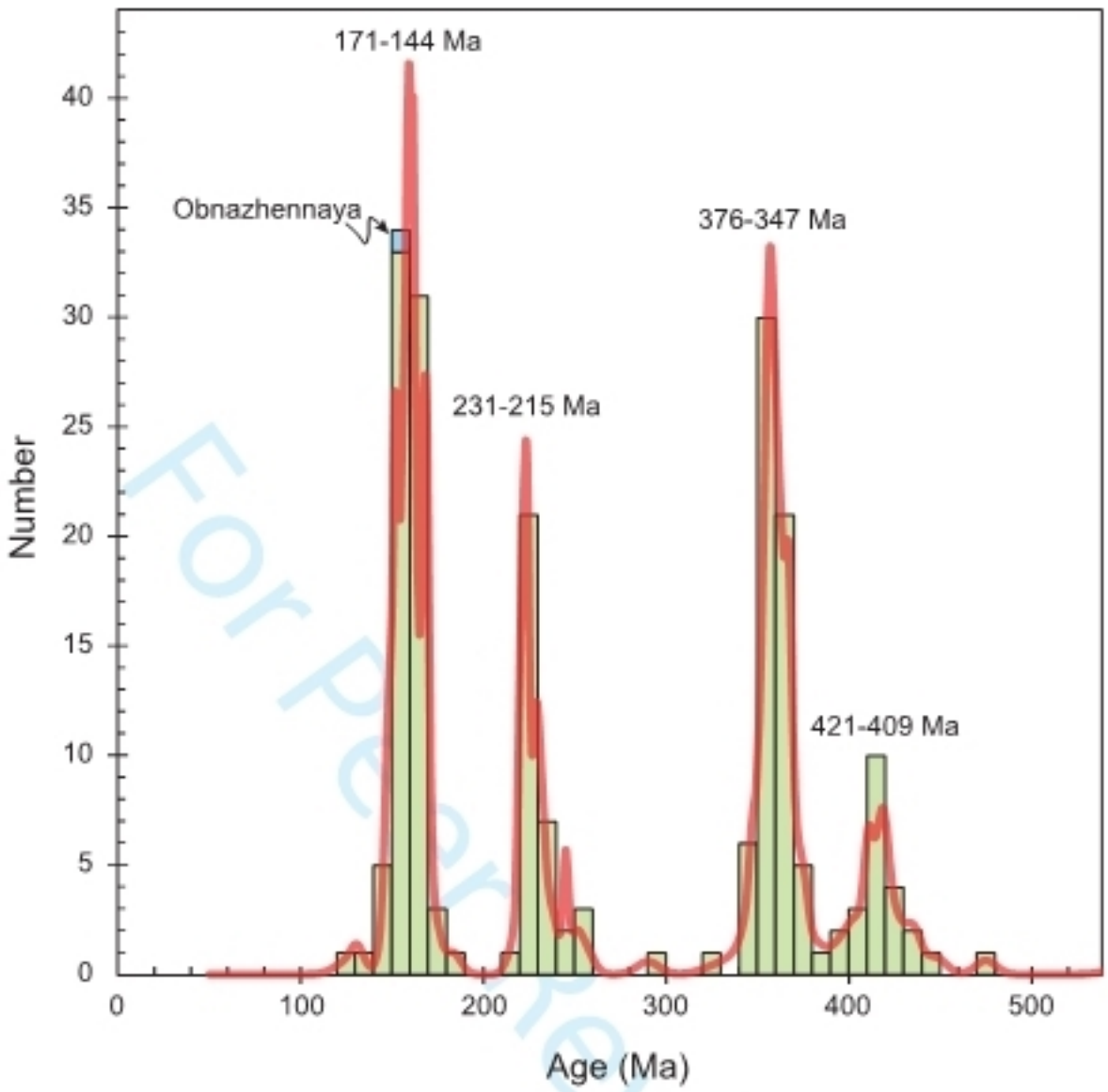

Fig. 5

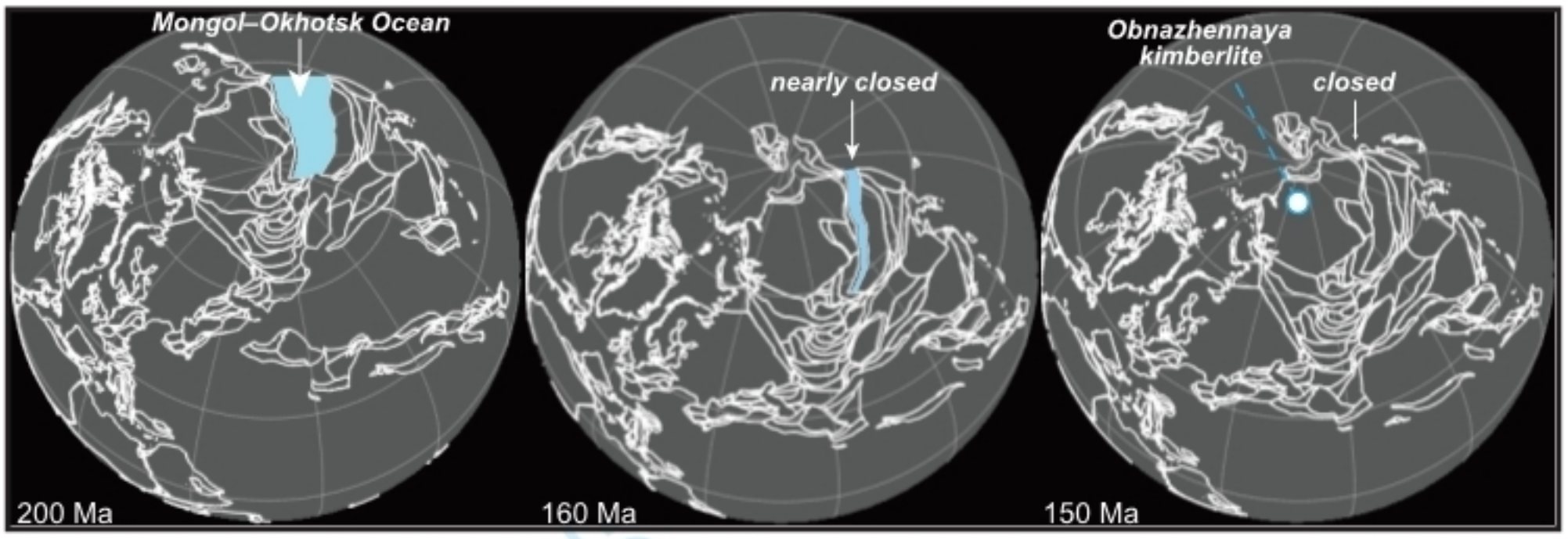

Fig.6

Supp. Table 1 SIMS U-Pb ages of perovskites from the Obnazhennaya kimberlite pipe

Sample	U (ppm)	Th (ppm)	Th/U	Pb (ppm)	Isotope ratio uncorrected				^{207}Pb correction SK model age (Ma)
					$^{238}U/^{206}Pb$	error(%)	$^{207}Pb/^{206}Pb$	error(%)	
obn7-191@01	31.61	57.57	1.82	0.11	27.6888	7.0	0.2778	0.7	164.0 ± 12.1
obn7-191@02	19.96	38.17	1.91	dl	27.4813	2.9	0.3342	0.5	148.9 ± 6.7
obn7-191@03	29.85	55.82	1.87	0.08	30.2655	3.4	0.2840	0.3	148.5 ± 6.3
obn7-191@04	29.58	54.22	1.83	0.03	29.2636	3.1	0.2846	0.7	153.4 ± 6.2
obn7-191@05	31.08	56.92	1.83	0.11	29.1171	2.9	0.2784	0.3	155.8 ± 5.9
obn7-191@06	35.86	67.13	1.87	0.14	29.7974	3.0	0.2710	0.4	154.3 ± 5.9
obn7-191@07	29.18	56.81	1.95	0.03	30.1906	3.0	0.2887	0.7	147.6 ± 5.9
obn7-191@08	27.69	54.98	1.99	0.02	29.8272	3.1	0.3013	0.9	146.0 ± 6.2
obn7-191@09	30.83	61.75	2.00	0.09	28.8092	3.3	0.2890	0.6	154.5 ± 6.5
obn7-191@10	34.66	59.13	1.71	0.16	30.1072	3.3	0.2711	0.5	152.6 ± 6.2
obn7-191@11	31.12	58.34	1.87	0.05	29.1072	3.0	0.2840	0.6	154.3 ± 6.1
obn7-191@12	29.78	60.55	2.03	dl	28.6386	2.7	0.2981	0.6	152.9 ± 6.0
obn7-191@13	28.26	55.59	1.97	0.03	29.5765	3.1	0.2903	0.8	150.2 ± 6.1
obn7-191@14	29.73	59.06	1.99	dl	29.5750	3.1	0.2898	0.6	150.4 ± 6.2
obn7-191@15	29.00	57.44	1.98	0.04	29.2169	3.1	0.2954	0.7	150.7 ± 6.2
obn7-191@16	28.56	53.64	1.88	0.12	30.4295	3.1	0.2730	0.6	150.5 ± 5.9
obn7-191@17	31.86	62.14	1.95	0.13	28.6589	2.9	0.2796	0.6	158.0 ± 6.1
obn7-191@18	33.69	60.10	1.78	0.07	30.3758	3.2	0.2771	0.7	149.7 ± 6.1
obn7-191@19	28.97	59.36	2.05	dl	29.0355	3.2	0.2963	0.3	151.3 ± 6.4
obn7-191@20	26.76	49.15	1.84	0.16	29.8938	3.0	0.2775	0.9	152.0 ± 5.9
obn7-191@21	27.78	56.53	2.03	0.04	28.9812	3.1	0.3010	0.6	150.4 ± 6.4
obn7-191@22	25.84	52.18	2.02	dl	28.3171	3.1	0.3080	0.6	151.9 ± 6.5
obn7-191@23	30.07	59.06	1.96	0.08	28.7967	3.2	0.2916	0.8	153.9 ± 6.5
obn7-191@24	23.97	47.65	1.99	dl	29.0819	3.1	0.3160	1.0	145.7 ± 6.4
obn7-191@25	28.36	59.22	2.09	0.07	28.7917	2.7	0.2913	0.8	154.0 ± 5.9

dl: detection limit

Supp. Table 2 LA-ICPMS U-Pb ages of rutile from eclogite xenoliths of the Obnazhennaya kimberlite

Comments	U ppm	$^{207}Pb/^{235}U$	2s	$^{206}Pb/^{238}U$	2s	$^{207}Pb/^{206}Pb$	2s	^{207}Pb-corr	2s
OBN_1_1	6.2	0.176	0.008	0.025	0.001	0.052	0.002	157.1	4.9
OBN_1_2	6.1	0.177	0.007	0.025	0.001	0.052	0.002	156.0	4.9
OBN_1_3	6.7	0.173	0.007	0.024	0.001	0.053	0.002	154.6	4.8
OBN_1_4	6.8	0.175	0.006	0.025	0.001	0.053	0.002	155.7	4.9
OBN_1_5	6.8	0.178	0.008	0.025	0.001	0.053	0.002	156.1	4.9
OBN_2_1	1.2	0.224	0.022	0.025	0.001	0.064	0.006	157.0	5.5
OBN_3	6.3	0.186	0.008	0.025	0.001	0.054	0.002	157.0	4.8
OBN_4	3.9	0.172	0.010	0.024	0.001	0.053	0.003	151.5	5.1
OBN_5	5.7	0.171	0.008	0.024	0.001	0.051	0.003	153.0	4.9
OBN_6_1	4.1	0.183	0.008	0.025	0.001	0.055	0.003	156.0	5.0
OBN_6_2	3.7	0.189	0.008	0.025	0.001	0.055	0.002	155.6	4.9
OBN_7	3.9	0.171	0.009	0.024	0.001	0.053	0.003	151.2	4.9
OBN_8_1	6.3	0.186	0.009	0.024	0.001	0.057	0.003	148.7	4.6
OBN_8_2	6.2	0.177	0.007	0.024	0.001	0.053	0.002	150.7	4.7
OBN_9	6.7	0.181	0.009	0.024	0.001	0.055	0.003	150.8	4.7
OBN_10	1.1	0.205	0.017	0.025	0.001	0.060	0.005	156.6	6.6
OBN_11_1	3.6	0.277	0.015	0.025	0.001	0.080	0.004	155.9	5.3
OBN_11_2	3.8	0.184	0.010	0.024	0.001	0.055	0.003	154.3	4.9